doi:10.1093/brain/aws162 Brain 2012: 135; 2416–2427 | 2416

BRAIN
A JOURNAL OF NEUROLOGY

Diencephalic–mesencephalic junction dysplasia: a novel recessive brain malformation

Maha S. Zaki,[1] Sahar N. Saleem,[2] William B. Dobyns,[3] A. James Barkovich,[4] Hauke Bartsch,[5] Anders M. Dale,[5] Manzar Ashtari,[6,7] Naiara Akizu,[8] Joseph G. Gleeson[8] and Ana Maria Grijalvo-Perez[8]

1 Department of Clinical Genetics, Division of Human Genetics and Genome Research, National Research Centre, Cairo 12311, Egypt
2 Department of Radiology, Cairo University, Cairo, Egypt
3 Department of Paediatrics, Seattle Children's Research Institute, Seattle, WA 98195-6320, USA
4 Department of Radiology and Biomedical Imaging, University of California, San Francisco, 94143, USA
5 Multimodal Imaging Laboratory (MMIL), Departments of Radiology and Neurosciences, University of California, San Diego, 92093 USA
6 Diffusion Tensor Image Analyses and Brain Morphometry Centre, Children's Hospital of Philadelphia, Philadelphia, PA 19104, USA
7 Department of Radiology, Children's Hospital of Philadelphia, Philadelphia, PA 19104, USA
8 Neurogenetics Laboratory, Howard Hughes Medical Institute, Department of Neurosciences and Paediatrics, Rady Children's Hospital, University of California, San Diego, 92093 USA

Correspondence to: Dr Maha S. Zaki,
Department of Clinical Genetics,
Division of Human Genetics and Genome Research,
National Research Centre,
El-Tahrir Street,
Dokki,
Cairo 12311,
Egypt
E-mail: dr_mahazaki@yahoo.com or mszaki60@internetegypt.com

We describe six cases from three unrelated consanguineous Egyptian families with a novel characteristic brain malformation at the level of the diencephalic–mesencephalic junction. Brain magnetic resonance imaging demonstrated a dysplasia of the diencephalic–mesencephalic junction with a characteristic 'butterfly'-like contour of the midbrain on axial sections. Additional imaging features included variable degrees of supratentorial ventricular dilatation and hypoplasia to complete agenesis of the corpus callosum. Diffusion tensor imaging showed diffuse hypomyelination and lack of an identifiable corticospinal tract. All patients displayed severe cognitive impairment, post-natal progressive microcephaly, axial hypotonia, spastic quadriparesis and seizures. Autistic features were noted in older cases. Talipes equinovarus, non-obstructive cardiomyopathy and persistent hyperplastic primary vitreous were additional findings in two families. One of the patients required shunting for hydrocephalus; however, this yielded no change in ventricular size suggestive of dysplasia rather than obstruction. We propose the term 'diencephalic–mesencephalic junction dysplasia' to characterize this autosomal recessive malformation.

Keywords: diencephalon; mesencephalon; mental retardation; brainstem malformation; brain wiring

Abbreviations: DMJ = diencephalic–mesencephalic junction; DMJD = diencephalic–mesencephalic junction dysplasia

Received February 6, 2012. Revised April 27, 2012. Accepted May 4, 2012

Introduction

Defects in brain development often result in structural anomalies that are identifiable on MRI. In addition to the well-known cortical dysplasias, a range of brainstem dysplasias has been described, which, due to the intricate anatomy, require more detailed structural analysis. These include pontocerebellar hypoplasia, Joubert's syndrome, pontine tegmental cap dysplasia and horizontal gaze palsy with progressive scoliosis (Barkovich *et al*., 2009). Since the brainstem is a site of cranial nerve nuclei, as well as a decussation and transit for most well defined ascending and descending tracts, these defects are frequently associated with unique signs and symptoms or altered tractography (Engle, 2010).

During embryogenesis, with induction of a combination of signals, an early regionalization or patterning of the neural tube along the anterior–posterior axis (the rostral–caudal axis) occurs, leading to a series of three anatomically defined vesicles at the rostral end. These three vesicles are the prosencephalon (forebrain), mesencephalon (midbrain) and rhombencephalon (hindbrain). Subsequently, the prosencephalon divides into the rostral telencephalon (cerebrum) and caudal diencephalon (thalami), whereas the rhombencephalon divides into the rostral metencephalon (pons and cerebellum) and caudal myelencephalon (medulla oblongata). The diencephalic–mesencephalic junction (DMJ) and the mesencephaic–rombencephalic junction (also known as the midbrain–hindbrain junction) act as important signalling centres during embryonic development. This was demonstrated in a series of experiments in which midbrain–hindbrain junction was grafted into forebrain, resulting in ectopic induction of midbrain tissue, and based upon this 'organizing activity' was named the isthmic organizer (IsO) (Martinez *et al*., 1991). Fgf8 is probably the main isthmic organizer signalling molecule, as ectopic Fgf8 protein can mimic its organizer activity (Martinez *et al*., 1999).

The mechanisms resulting in the positioning of the DMJ are not fully understood but probably mirror those of the midbrain–hindbrain junction. In animal models, maintenance of the DMJ requires both the presence of a specified midbrain and a functional midbrain–hindbrain junction (Scholpp *et al*., 2003). Like the midbrain–hindbrain junction, the DMJ is probably formed under the genetic influence of secreted fibroblast growth factor 8 (*FGF8*) (Nakamura and Watanabe, 2005), which regulates the anterior–posterior expression of the engrailed (En) and Paired box (Pax) transcription factors. Changes in expression of these genes shifts the DMJ boundary caudally (more Pax6) or rostrally (more En2 and En3), whereas combined loss of both En2/En3 and Fgf8 leads to complete loss of midbrain identity, resulting in fusion of the forebrain and the hindbrain primordia (Scholpp *et al*., 2003). Human defects of the DMJ are poorly understood.

We describe six familial cases with a novel pattern of malformation at the DMJ. We propose the term 'butterfly sign' to describe the MRI appearance of the midbrain on axial images, which may be a pathognomonic finding in this condition. Additionally, we demonstrate the absence of evident corticopontine/corticospinal tract fibres based upon diffusion tensor imaging in two affected individuals. The pedigree structure suggests that diencephalic–mesencephalic junction dysplasia (DMJD) is likely to be inherited in a recessive fashion. We hypothesize that these cases represent a novel brain malformation syndrome with a defect in organization of the DMJ.

Materials and methods

Patient ascertainment

The patients were enrolled in a sequential fashion in the Neurogenetics Clinic at National Research Centre, Cairo, Egypt, between December 2010 and November 2011, from participants meeting inclusion criteria for brain malformations in this institutional review board-approved study. Signed consent for study entry was provided to the National Research Centre and the University of California, San Diego Ethics Board. Routine medical records, history, physical and neurological examination as well as brain imaging studies were evaluated.

Image processing

All studies were performed using field strengths of 1.5 T superconducting magnet (Intera; Philips Medical Systems) at the Radiology Department, Cairo University and sagittal and coronal T_1 and/or T_2 images, 3–5 mm slice thicknesses were obtained in all patients. Images were corrected for non-linear warping caused by non-uniform fields created by the gradient coils (Jovicich *et al*., 2006). Image intensities were corrected for spatial sensitivity inhomogeneities in the 8-channel head coil by normalizing with the ratio of a body coil scan to a head coil scan. Diffusion tensor images were acquired and processed in DICOM format in two of the affected individuals (Patients DMJD-1592-2 and -3), with further segmentation according to the following sequence. Two T_1-weighted images were rigid body registered to each other, averaged and reoriented into a common space, similar to alignment based on the anterior commissure–posterior commissure line.

For diffusion image preprocessing the following steps were performed: (i) head motion between scans was removed by rigid body registration between the $b = 0$ images of each diffusion-weighted scan; (ii) within-scan motion was removed by calculating diffusion tensors, synthesizing of diffusion-weighted volumes from those tensors, and rigid body registering each data volume to its corresponding synthesized volume; (iii) image distortion in the diffusion-weighted volumes caused by eddy currents was minimized by non-linear optimization; and (iv) images were resampled using cubic interpolation to 1.875 mm^3 isotropic voxels.

Surface reconstruction of the brain, brainstem and ventricles was analysed in one of the patients (Patient DMJ-1592-2) and compared with an age-matched control. Volumetric analysis of both the cortex as well as brainstem was performed and those data were compared with the National Institutes of Health volumetric database from healthy individuals aged 4–18 years (BDCG, 2012). The segmentation of the brainstem and the surface reconstruction was performed using Amira software (Visage Imaging Inc.). The diffusion tensor images were registered against the T_1 MRI. The directionally encoded images (coloured orientation images) were computed from the gradient-weighted images (http://meteoreservice.com/PDFs/JMRI_DTI.PDF) and encode the main diffusion direction for each voxel. Fractional anisotropy analysis was performed according to standard methods (Hagler *et al*., 2009).

Homozygosity mapping was performed as described (Seelow *et al*., 2009) using output from exome sequencing results (BAM files) from each of two affected individuals from Family DMJD-1592. Parameters were set to analyse blocks of 200 sequential markers and blocks only

counted if more than 50 contiguous homozygous markers were identified.

Results

Family DMJD-1592

This family presented with two affected males for evaluation of global developmental delay. Parents were healthy first cousins and had an older asymptomatic female child (Fig. 1). Family history was unremarkable. The paternal and maternal ages were 28 and 23 years, respectively.

The older affected male (Patient DMJD-1592-2) was 4-years-old at the time of his last assessment (Table 1). The pregnancy was reportedly uneventful and he was delivered vaginally at term after a prolonged labour, was cyanotic at birth with an Apgar score of 6 at 10 min. He remained at the neonatal intensive care unit for 1 week and discharged in good condition with average sucking, strong cry and good antigravity power for age. At 22 days old, he developed focal seizures, which at times evolved into secondary generalized seizures that were initially well controlled with phenobarbital. Parents noted severe delay in all developmental milestones, prompting an initiation of physiotherapy at 7 months of age with minimal improvement.

Seizures became more frequent, so was switched to a regimen of carbamazepine and valproate, which decreased seizure frequency. History of vasomotor instability on cold weather and recurrent unexplained prolonged fevers were recorded. On general examination, the patient was able to sit with support, had evident autistic features and was able to vocalize but had no words. He had marked microcephaly and specific facial features including an unusual hair whorl, facial hirsutism (more prominently over his forehead), long bushy eyebrows, broad prominent nasal root, epicanthal folds, long linear palpebral fissures, strabismus, long flat philtrum, V-shaped upper lip with prominent vermilion, prominent central incisors, recessed mandible, posteriorly rotated large ears and short neck. No abnormalities of his upper and lower extremities were noted, no hepatosplenomegaly or neurocutaneous stigmata and the rest of the general examination was unremarkable. He displayed a limited ability to track to light but the rest of his cranial nerves were intact. There was marked axial hypotonia with prominent head lag and minimal ability to lift his head. He was unable to reach or grasp for objects. Spasticity predominated in both upper and lower extremities with brisk deep tendon reflexes, and response to painful stimuli was appropriate. Current weight was 13 kg [standard deviation (SD) −1.9], length 87 cm (SD − 3.2) and head circumference 43 cm (SD − 6.1). Diagnostic workup to date included a high-resolution karyotype, extended metabolic screening, fundoscopic exam, visual-evoked potentials and brainstem auditory-evoked potentials, all normal. EEG revealed bilateral interictal epileptiform discharges over the temporoparietal regions.

The younger affected individual (Patient DMJD-1592-3) was delivered via elective caesarean section. He was considered healthy at birth with weight 3 kg (SD − 1), length 51 cm (SD + 0.5) and head circumference 34.5 cm (SD − 0.8). At 18 days of post-natal age he developed left sided focal seizures, which were prolonged requiring intravenous diazepam. He was initiated on phenobarbital and seizures were subsequently well controlled on monotherapy levetiracetam. At 60 days of life, he was alert, could follow light and track objects in all directions of gaze. Moro reflex was present but not stepping reflexes. His weight was 5.5 kg (SD + 0.3), length was 57 cm (mean) and head circumference was 37 cm (mean) with very small anterior fontanel. On neurological examination, he had mild truncal hypotonia and otherwise normal tone in both upper and lower extremities. Patient was re-evaluated at the age of 3.5 months. He had gained weight (7 kg) (SD + 0.8) and length (63 cm) (mean) but there was cessation of head growth 37 cm (SD − 1.8) with closed anterior fontanel. The patient had similar facial features as his brother. Neurologically, the patient was fairly able to support his head but there was increased tone in upper and lower extremities with persistent hand fisting. Strabismus was first noted at the age of 6 months and an exaggerated startle reflex was still prominent. Diagnostic evaluations were the same for the older sibling and were all within normal limits. EEG showed recurrent interictal bilateral epileptiform discharges located over the mid-parietal regions.

Family DMJD-1825

A female child (Patient DMJD-1825-2) from an unrelated consanguineous Egyptian family was noted to have a similar pattern of DMJD abnormality on MRI studies. Parents were asymptomatic first cousins aged 29 years old (father) and 23 years old (mother). They had a symptomatic older male child that died at 14 months (Subject DMJD-1825-1). The family denied any complications during pregnancy, labour or delivery. The child presented with severe developmental delay. She was diagnosed with hydrocephalus in the first month of life and a ventriculoperitoneal shunt was performed at 2 weeks of life. However, in spite of the surgery, subsequent neuroimaging studies showed severe enlargement of the lateral ventricles with a normal size fourth ventricle suggesting dysplasia rather than obstruction. At 30 days of post-natal age, she had new onset of tonic seizures and was started on valproate with fair seizure control. She was 17 months old at the time of her last evaluation. On exam she was severely microcephalic with a head circumference of 38 cm (SD − 6.2), and had failure to thrive with weight of 6.5 kg (SD − 4.2) and length of 71 cm (SD − 3). The patient had specific facial features such as long bushy eye brows, broad prominent nasal root, epicanthal folds, long linear palpebral fissures, long flat philtrum, V-shaped thin upper lip, retracted mandible, posteriorly rotated large ears and short neck. In addition she was noted to have bilateral talipes equinovarus at birth requiring repeated casting. A short systolic murmur was also noticed and accordingly, she had an evaluation with an ECG that showed mild non-obstructive hypertrophic cardiomyopathy.

Neurological examination showed spastic quadriparesis with poor head control and truncal hypotonia. She was non-verbal and non-ambulatory. She had vasomotor instability and episodic unexplained fevers. Karyotype, fundoscopy, brainstem auditory-evoked potentials, visual-evoked potentials and metabolic testing

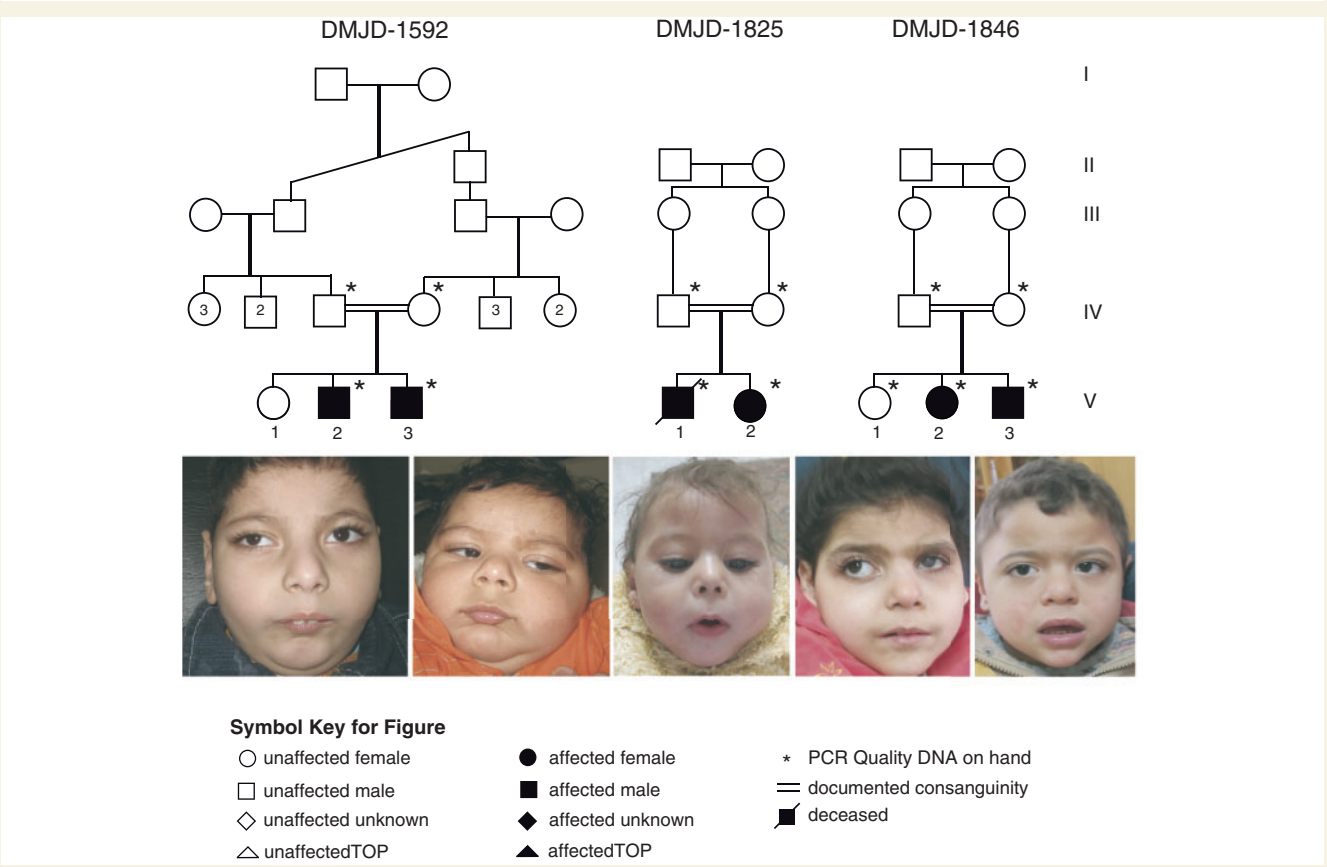

Figure 1 Pedigree of Families DMJD-1592, DMJD-1825 and DMJD-1846. Facial images demonstrate shared features of bushy eyebrows, hairy forehead, broad prominent nasal root, long flat philtrum and V-shaped upper lip.

were all normal. EEG showed right frontotemporal interictal epileptiform discharges extending to the left cerebral hemisphere associated with diffuse generalized slowing.

Although deceased at the time of evaluation, the family provided records on the male Subject DMJD-1825-1, including imaging studies that allowed us to determine that he had an identical brain malformation as the younger sibling. He had onset of seizures within the neonatal period as well a similar neurological examination extracted from medical records as available and from old photographs. While there was ventriculomegaly, shunting had not been performed.

Family DMJD-1846

Two affected female and male siblings derived from healthy first cousin parents, 34-year-old father and 30-year-old mother and had normal older female sibling (Fig. 1). The older affected girl (Patient DMJD-1846-2) was 4 years old at the time of her evaluation. Pregnancy history was irrelevant except for placental atrophy noted late in pregnancy required elective caesarean section. At birth, patient had average weight, height and head circumference and was healthy. Focal seizures were evident at the age of 1 month, involving the left side of the body with deviation of the eyes controlled on phenobarbital. At the age of 5 months, parents noted haziness of left eye uncovered by ophthalmological investigations as persistent hyperplastic primary vitreous with secondary glaucoma. She was maintained on local treatment to reduce the intraocular pressure. No milestones of development were achieved. Myoclonic seizures superimposed on focal seizures were inadequately treated with triple drug therapy involving valproate, levetiracetam and clonazepam. On examination, the patient was severely delayed, autistic and had failure to thrive. Her weight was 8.5 kg (SD – 4.8), height 89 cm (SD – 2.5) and head circumference 39 cm (SD – 8.7). She could minimally support the head and visually track objects with the unaffected eye but had no vocalization. She had bushy eyebrows, hairy forehead, broad prominent nasal root, strabismus, trichomegaly, long flat philtrum, V-shaped thin upper lip, broad chin and posteriorly rotated large ears. No skeletal deformities were present. History of vasomotor instability, recurrent unexplained fever, and persistent fungal infection of nails was prominent. General examination was non-contributory, and neurological examination revealed severe axial hypotonia, spastic lower limbs with clear asymmetry showing more severe affectation of the left side of the body. Sensation was intact. Investigations identical to other affected individuals were within normal limits. EEG revealed right temporo-parieto-occipital epileptogenic activity with a tendency to generalization.

Table 1 Clinical and neurophysiology data

Patient ID	DMJD-1592-2	DMJD-1592-3	DMJD-1825-1	DMJD-1825-2	DMJD-1846-2	DMJD-1846-3
Male/female	Male	Male	Male	Female	Female	Male
Ethnic origin	Egyptian	Egyptian	Egyptian	Egyptian	Egyptian	Egyptian
Parental consanguinity	+	+	+	+	+	+
Age (years;months)	4;4	0;7	Died at 1;2	1;5	4	2;5
OFC (SD) at birth, cm	33 (−1.5)	34.5 (−0.8)	33 (−1.5)	33 (−0.6)	33.8 (−0.8)	34 (−1)
Weight (SD) at birth, kg	2.700 (−1.3)	3 (−1)	2 (−3)	3.4 (mean)	3 (−0.5)	3.2 (−0.5)
Length (SD) at birth, cm	50 (mean)	51 (+0.5)	48 (−1)	47 (−1.2)	49 (0.3)	50 (mean)
Early neonatal history	Incubated for 7 days	–	Incubated for 30 days	Progressive head enlargement, shunt operation at 14 days	–	Incubated for 3 days
Current OFC (SD), cm	43 (−6.1)	37 (−1.8)	38 at 1 year (−5.3)	38 (−6.2)	39 (−8.7)	45 (−3.2)
Weight (SD), kg	13 (−1.9)	7 (+0.8)	6 at 1 year (−2.6)	6.5 (−4.2)	8.5 (−4.8)	14 (+0.5)
Length (SD), cm	87 (−3.2)	63 (0)	70 at 1 year (−2.4)	71 (−3)	89 (−2.5)	85 (−0.8)
Cranial nerve findings	Recurrent dysphagia, able to track objects and respond to sounds, strabismus	Able to track objects and respond to sounds, strabismus	Recurrent dysphagia, not able to track objects	Recurrent dysphagia, can track objects	Recurrent dysphagia, minimal tracking of objects, strabismus	Able to track objects and respond to sounds, strabismus
Speech	Delayed, vocalizes non-specific	Babbles	Non-verbal	Non-verbal	Non-verbal	Vocalizes non-specific
Autistic features	+	–	–	+	+	+
Gait	Non-ambulatory	Non-ambulatory	Non-ambulatory	Non-ambulatory	Non-ambulatory	Non-ambulatory
Head lag	+/No independent head support	+/Minimal head support	+/No independent head support	+/Minimal head support	+/Minimal head support	+/Frequent head support
Ataxia	Absent	Absent	Absent	Absent	Absent	Absent
Pyramidal tract signs	Spastic quadriparesis/ hyper-reflexia	Mild spasticity, hyper-reflexia, maintains grasped hands	Spastic quadriparesis	Spastic quadriparesis/ hyper-reflexia	Spastic quadriparesis/ hyper-reflexia	Mild spasticity, hyper-reflexia, maintains grasped hands
Seizures onset/type	22 days/partial with secondary generalization	18 days/partial	7 days/tonic	30 days/tonic	30 days/partial and myoclonic	4 months/partial, and myoclonic
Seizures: controlled/ treatment	Fairly controlled on phenobarbital then carbamazepine and valproate	Controlled on levetiracetam	Fairly controlled on phenobarbital and valproate	Fairly controlled on valproate	Fairly controlled on valproate, levetiracetam and clonazepam (still daily few myoclonic fits)	Fairly controlled on valproate and levetiracetam
Vasomotor instability/recurrent unexplained fever	+	–	+	+	+	+
External dysmorphia	+ Specific facies and short neck	+ Specific facies and short neck	+ Specific facies/bilateral talipes equinovarus	+ Specific facies/bilateral talipes equinovarus operated	+ Specific facies/hazy left eye	+ Specific facies
Other exam findings	–	–	–	Short systolic flow murmur over pericardium	Unilateral persistent hyperplastic primary vitreous and glaucoma	–
Karyotype	46, XY	46, XY	46, XY	46, XX	46, XX	46, XY
Metabolic testing	Negative	Negative	Negative	Negative	Negative	Negative
EEG	Bilateral epileptiform discharges over the temporoparietal region	Mild bilateral mid-parietal epileptiform activity	N/A	Right frontotemporal epileptiform discharges extending to the left hemisphere and generalized slowing	Right tempro-parieto-occipital epileptogenic activity with secondary generalization	Right centro-temporal spikes with tendency to generalization
Fundus examination	Normal	Normal	Normal	Normal	Normal right eye/abnormal in left eye	Normal
VEP/BAEP	Normal/normal	Normal/normal	Normal/normal	Normal/normal	Normal right eye and abnormal in left eye/normal	Normal/normal
Echocardiography	Normal	Normal	N/A	Non-obstructive hypertrophic cardiomyopathy	Normal	Normal
Neuroimaging findings other than DMJD	Bilateral ventriculomegaly, CCH	Mildly dilated lateral ventricles, CCH	ACC, hugely dilated lateral ventricles, thin cerebral mantle, cerebellar vermis hypoplasia	ACC, hugely dilated lateral ventricles in spite of shunt operation, thin cerebral mantle, cerebellar vermis hypoplasia	CCH, ventriculomegaly, with asymmetry and mild atrophic right cerebral hemisphere	CCH, ventriculomegaly

ACC = agenesis of the corpus callosum; BAEP = brainstem auditory-evoked potentials; CCH = corpus callosum hypoplasia; N = normal; N/A = not available; OFC = occipital–frontal circumference; VEP = visual-evoked potentials.

The younger affected individual (Patient DMJD-1846-3) is a 2.5-year-old male patient delivered by caesarean section. He was admitted to neonatal intensive care unit for 3 days to stabilize his condition due to tachypnea. Neonatal period and early infancy were unremarkable. Focal seizures with secondary generalization developed at the age of 4 months controlled on valproate. Delayed milestones of development were evident and intensive physical and stimulation therapy were started at the age of 9 months. Recurrent myoclonic fits appeared at the age of 1 year and a second drug therapy with levetiracetam was introduced. On examination, the patient had general appearance less severe than his affected sister. He could sit with support, was unable to use his hands, had prominent autistic features and grinding movement and could vocalize without words. His weight was 14 kg (SD + 0.5), height was 85 cm (SD − 0.8) and head circumference 45 cm (SD − 3). His faces showed long straight eyebrows, broad prominent nasal root, straight palpebral fissures, strabismus, long flat philtrum, V-shaped upper lip with prominent vermilion and posteriorly rotated large ears. Neurologically, mild axial hypotonia, symmetric limbs hypertonia and brisk reflexes were present. Sensation was intact and no history of vasomotor instability or unexplained fever. Similarly, all investigations were irrelevant, fundoscopic examination of both eyes was normal and EEG showed right centro-temporal spikes with tendency towards generalization.

Imaging findings

MRI was obtained on all children. Non-contrast head CT was additionally available in half of the children. T_1/T_2 axial MRI sequences show thickening and shortening of the midbrain on the rostro-caudal axis with a poorly defined junction between the diencephalon and the mesencephalon. Abnormal morphology of both the ventral as well as dorsal aspects of the midbrain was noted. The contour of the midbrain in transverse section exhibited a unique and distorted pattern, with an enlarged dorso-ventral axis and a deeper than normal interpeduncular fossa (Figs 2 and 3). This fossa or cleft is contiguous with the third ventricle, and appears to represent a dorsal displacement of the caudal and posterior third ventricle. We propose the term 'butterfly sign' to describe the characteristically abnormal appearance of the DMJ in these six patients, which appears to be unique from any previously reported condition. On coronal sections, merger was noted between the midbrain and thalami as well as extension of the third ventricle into the midbrain. Rare and mostly supratentorial calcifications are seen on CT on both affected siblings of Family DMJ-1592 (data not shown).

Massively enlarged lateral ventricles were appreciated in both affected individuals from Family DMJD-1825 (Fig. 2). Both patients also displayed near complete absence of the corpus callosum, and therefore the ventriculomegaly might be more likely not to be due to aqueductal stenosis but rather abnormal white matter development (so-called 'colpocephaly'). Furthermore, the cerebral aqueduct appeared patent, arguing against obstructive hydrocephalus. Corpus callosal hypoplasia was also observed, albeit to a much less extent in the other four affected children presented here. In all six cases, the fourth ventricle was normal in size, and in Patient DMJD-1825-1 there was cerebellar vermis counter-clockwise rotation and hypoplasia.

Surface reconstruction of both the brainstem (Fig. 4) as well as the cortex was performed. No areas of cortical migrational abnormalities such as polymicrogyria or lissencephaly were noted on review of the cortical surface reconstruction images. Volumetric analysis was performed in Family DMJD-1592. Brainstem volume was estimated at 32.405 cm^3 (123.5% of healthy control) and the total cortical volume was 559.21 cm^3 (61.4% of healthy control), compared with the National Institutes of Health MRI study (BDCG, 2012).

The neuroanatomy at the level of DMJ was further delineated in two patients from Family DMJD-1592 including diffusion tensor imaging to generate fractional anisotropy maps (Fig. 5). On axial images, severely reduced axonal volume in all the major cortical descending pathways was evident. Most notable was at the level of the pons, where the vertically oriented medial lemniscus tract and the horizontally oriented pontine crossing track were visible. The corticopontine/corticospinal tract, which is usually well demarcated in the anterior part of the pons and evident in control images, was completely absent in both affected individuals, and region of interest mapping failed to delineate its course at levels below the insula. This observation suggests a defect in axonal pathfinding. It was not possible to differentiate between a complete absence of the corticopontine/corticospinal tract from the level of the cerebral cortex versus premature termination within the internal capsule.

Discussion

In this study, we describe six familial cases of a novel malformation at the DMJ in three consanguineous Egyptian families. None of the three families are related to one another, according to our knowledge, but we cannot exclude a common shared ancestor or founder mutation. It is likely that these three families depict a novel developmental brain disorder not previously classified. Although we propose that the affected individuals in these families are likely to have the same unique condition, there are some differences in the degree of ventriculomegaly, with Family DMJD-1825 showing dramatic ventriculomegaly not observed in either of the other two families. Therefore, at this time, it remains a possibility that these represent genetically distinct diseases with a similar unique brainstem malformation.

Findings similar to these have appeared in the published literature previously, but not as a distinct entity or with clarified inheritance pattern. We previously reported two cases of midbrain enlargement with midline hyperintensity, pontocerebellar hypoplasia and a hyperintense (T_2-positive) midline stripe extending from the interpeduncular cistern to the aqueduct (Barkovich *et al*., 2007). In these two cases, the midbrain showed some similarities in structure to those reported here, but were not identical. An additional case was identified in our subsequent report of the genetic classification for midbrain–hindbrain malformations (Barkovich *et al*., 2009), which we attributed to a posterior-to-anterior transformation at the level of the DMJ. In these previous cases, we observed

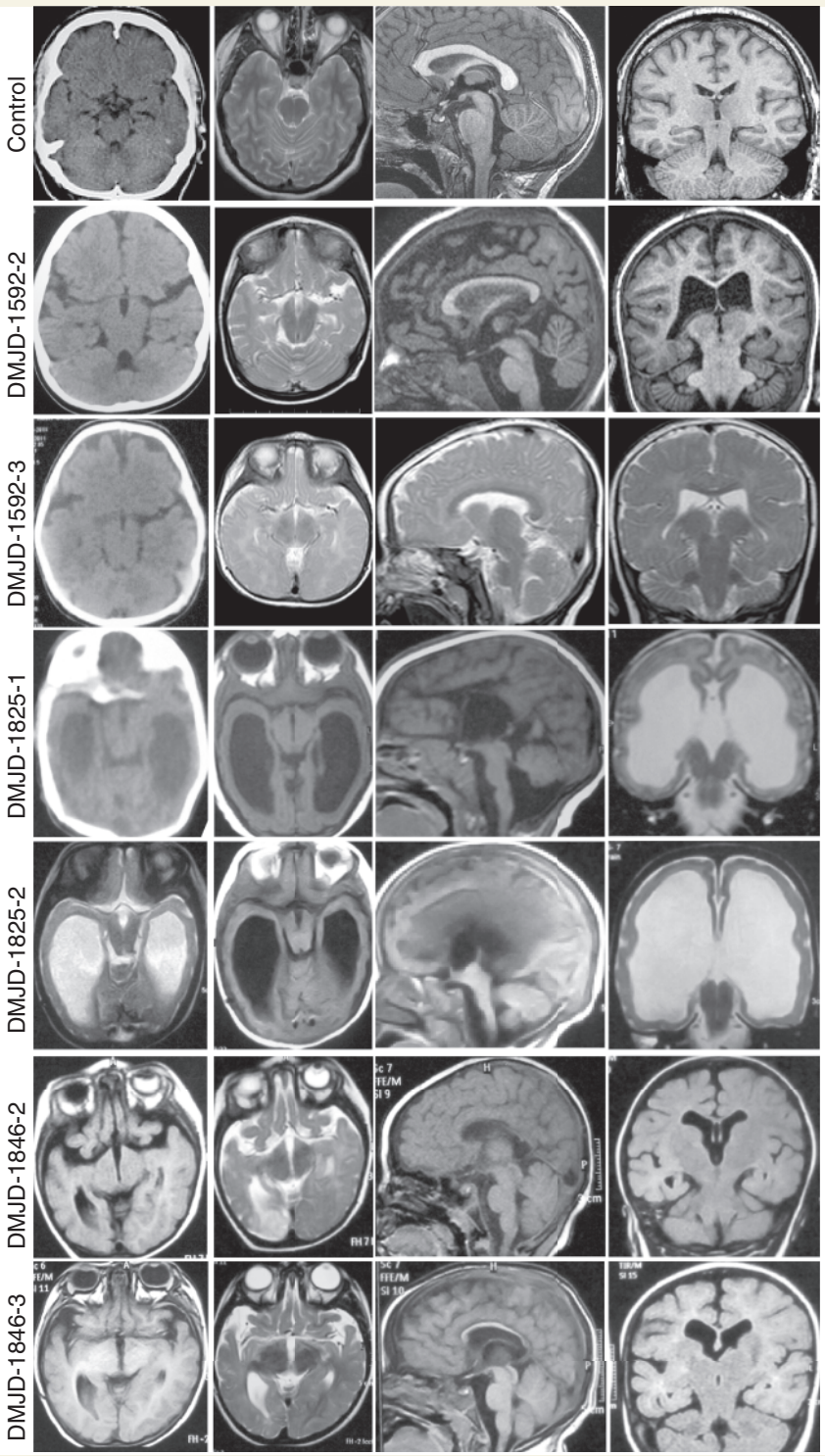

Figure 2 Structural brain images from each patient, showing the typical 'butterfly' appearance of the DMJ. *Top* row is aged-matched controls for comparison. All patients show some degree of ventriculomegaly and corpus callosum hypoplasia. Patient DMJD-1825-1 shows cerebellar vermis counter-clockwise rotation and hypoplasia. *From left to right*: Columns 1 and 2: axial CT (where available) or MRI at the level of the DMJ. Note the deep anterior midline cleft and elongated mesencephalon. Column 3: midline sagittal MRI showing corpus callosum hypoplasia. Column 4: coronal MRI showing corpus callosum hypoplasia and variable degrees of ventriculomegaly.

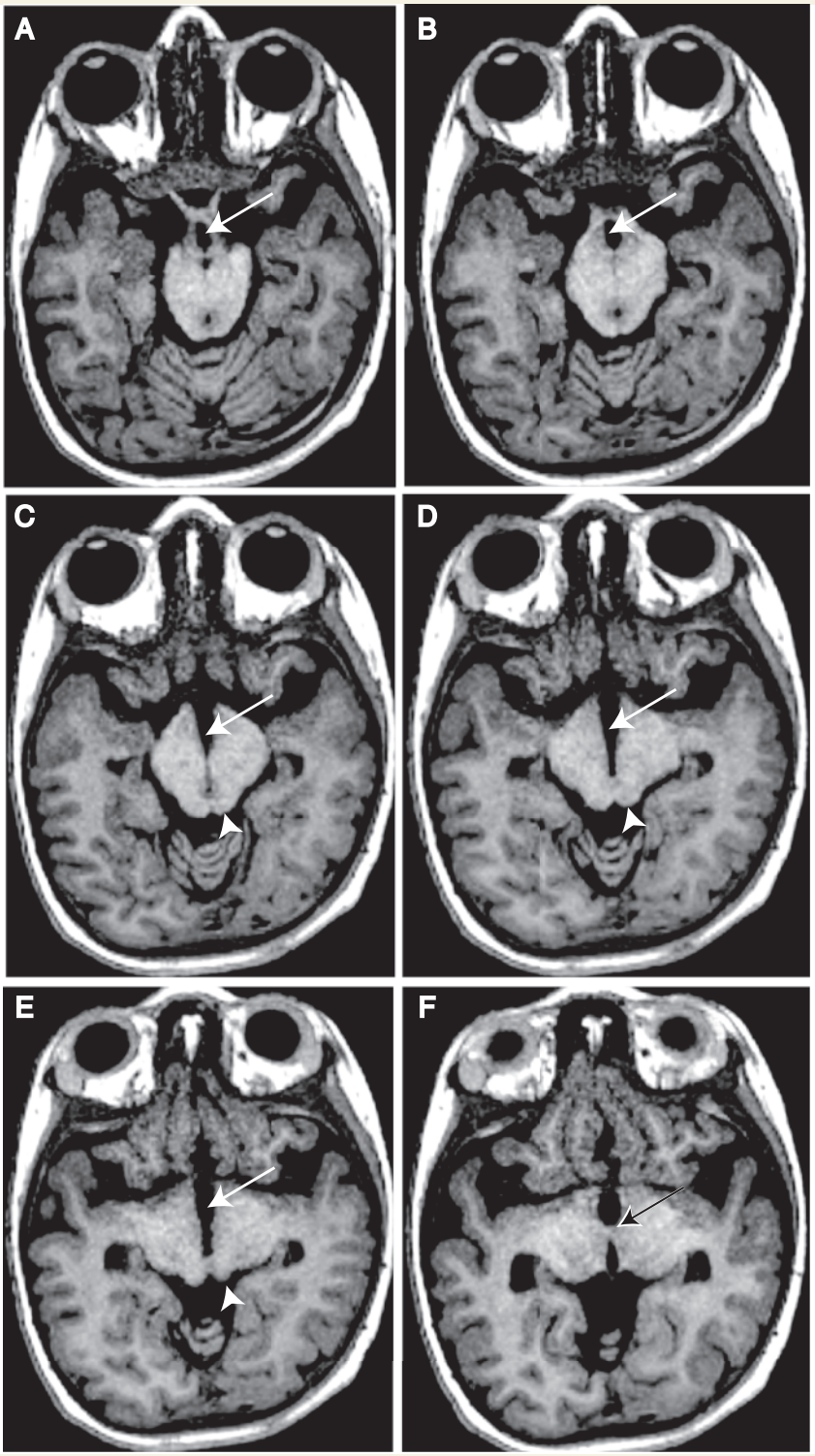

Figure 3 Key anatomical features of DMJD. T_1-weighted axial 1.2 mm thin sections from Patient DMJD-1592-2, demonstrating that the anterior midbrain cleft is continuous with the third ventricle. (**A** and **B**) Arrows indicate chiasmatic recess. (**A**) Optic track entering the midbrain. (**B**) Optic radiations coursing around midbrain. (**C** and **D**) Arrows indicate third ventricle extending posteriorly, producing the 'butterfly' sign. Arrowhead indicates inferior colliculi. (**E**) Arrow indicates third ventricle. Arrowhead indicates superior colliculi. (**F**) Arrow indicates massa intermedia (interthalamic adhesion), defining posterior limit of third ventricle.

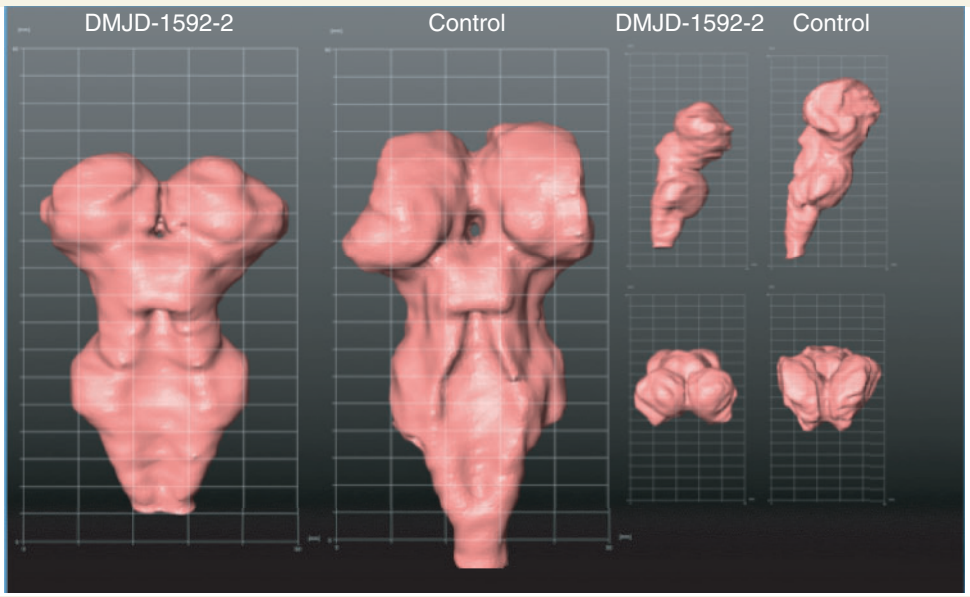

Figure 4 Three-dimensional reconstruction of the surface projection of brainstem from affected individual Patient DMJD-1592-2 compared with an age-matched control. Notice the brainstem is foreshortened, thalamus is inferiorly displaced to the level of the mesencephalon, and the DMJ is thickened. *Left*: posterior view. *Top right*: lateral view. *Bottom right*: top–down view.

extension of the third ventricle and other diencephalic features into the upper part of a thickened midbrain, similar to what was observed in mouse upon overexpression of *Pax6* or underexpression of *En1/Pax2* in the anterior mesencephalon (Nakamura and Watanabe, 2005). Whether these previously reported cases have the same genetic aetiology as the cases reported here will require identification of causative gene(s). Given the caudal shift of the DMJ and the interplay between the development of the DMJ and the midbrain–hindbrain junction, one might anticipate patterning defects of the midbrain–hindbrain boundary. It is therefore relevant that the affected individuals from Family DMJD-1825 showed cerebellar vermis hypoplasia.

DMJD joins a number of recessive brainstem developmental defects including pontocerebellar hypoplasia, Joubert's syndrome, pontine tegmental cap dysplasia and horizontal gaze palsy with progressive scoliosis, among others (Rossi *et al*., 2004; Barth *et al*., 2007; Cassandrini *et al*., 2010; Sattar and Gleeson, 2011). In each of these conditions, unique MRI appearance of the brainstem and/or cerebellum is evident, which allows for a refined patient classification. For instance, pontocerebellar hypoplasia due to mutations in the *TSEN54* gene shows a unique finding of flattening of the cerebellar hemisphere with relative sparing of the vermis producing a 'dragonfly-like' cerebellar pattern on coronal MRI (Namavar *et al*., 2011). Joubert's syndrome shows a 'molar-tooth' sign on axial images (Parisi, 2009), PTCH shows a unique bulge of the posterior brainstem into the fourth ventricle, and horizontal gaze palsy with progressive scoliosis shows a 'split pons' sign on axial MRI (Barkovich *et al*., 2009). The axial MRI in DMJD is highly unique, and appears to be clearly distinct from these other conditions, but additional work will be needed to substantiate these unique imaging findings.

Based upon these brainstem anatomical defects, we tested for fibre tract defects using diffusion tension imaging and found significant abnormalities in brain connectivity. Specifically, we noted abnormality in the continuity of the descending corticopontine/corticospinal tract. Given the limitation of diffusion tensor imaging, it was not possible to differentiate between a complete absence of this major tract from the cerebral cortex versus premature termination of the tract within the internal capsule. Additionally, it remains a formal possibility that the corticopontine/corticospinal tract originates normally but takes a sharp angle or projects in a different location, neither of which are possible to disprove using diffusion tensor imaging. Other developmental brain disorders display alterations in the corticopontine/corticospinal tract projections, specifically in Joubert's syndrome and horizontal gaze palsy with progressive scoliosis the corticopontine/corticospinal tract fails to decussate at the cervicomedullary junction at least in some patients (Yachnis and Rorke, 1999; Jen *et al*., 2004). In the case of mutations in *L1CAM*, humans have reduced corticospinal tract function (Dobson *et al*., 2001), whereas *L1cam* knockout mice show failed decussation and premature termination of the corticospinal tract at spinal levels (Cohen *et al*., 1998), and spasticity is a key feature. The spasticity displayed by our patients would be consistent with failed descending corticospinal tract projection, as this tract is critical for setting peripheral neuromotor tone. The specific mechanisms underlying such tractography defects are not known and will require future work.

Although our patients shared many dysmorphic facial features, we could not specify a distinctive syndromic pattern that would aide in diagnosis. We found post-natal progressive microcephaly, autistic features, seizures and spasticity are consistent features among our patients suggesting penetrant clinical stigmata of this malformation. Vasomotor instability and unexplained fever might

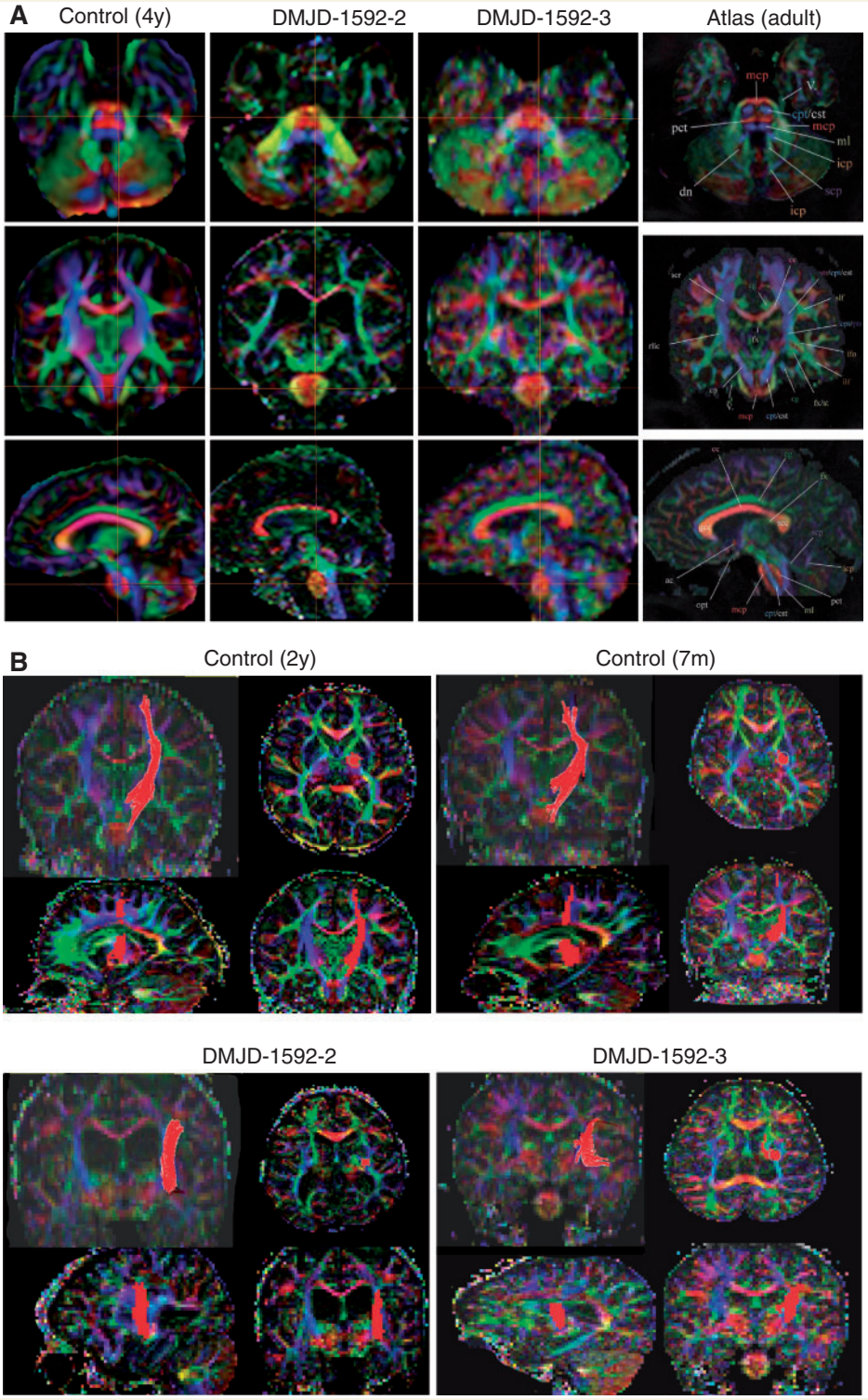

Figure 5 Disrupted corticospinal tract in DMJD. (**A**) Multiplane reconstruction with directional encoded colours from diffusion tension imaging of paediatric control, and two affected members in Family DMJD-1592 in comparison with MRI atlas of human white matter (Mori *et al*., 2011). *Top*: Axial plane in control shows corticopontine/corticospinal tracts evident in pons in blue (crosshairs), whereas neither patient has evident corticopontine/corticospinal tract. *Middle*: Coronal plate also shows corticopontine/corticospinal tract at crosshairs in control but absent in both patients. *Bottom*: Parasagittal plane also shows evident corticopontine/corticospinal tract in control, absent in patients. Crosshairs represent the relative plane of imaging for each of the images in the series for maximal registration correspondence. (**B**) Region of interest tractography of corticopontine/corticospinal tract fibre bundle (red) in each orientation from aged-matched control and the two affected members of Family DMJD-1592. Control shows the usual course of corticopontine/corticospinal tract, originating in the cortical motor area, lateral to the ventricle and then heading medially in the diencephalon/mesencephalon. Both patients show aberrant course of corticopontine/corticospinal tract, coursing laterally.

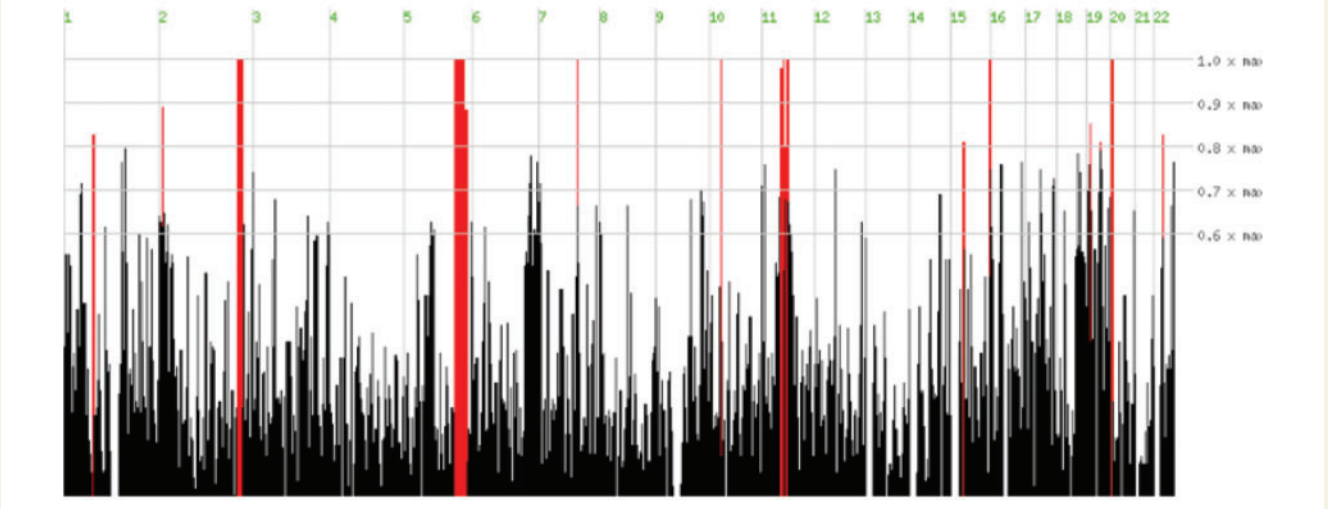

Figure 6 Homozygosity mapping results derived from comparison of exome sequencing of two affected individuals in Family DMJD-1592. The ~20 000 variants from each patient were plotted as a function of heterozygosity/homozygosity at each allele for each chromosome (*x*-axis). Red bars represent regions of homozygosity, which reach maximum significance (height of red bar) on chromosomes 2, 5, 7, 10, 11, 16 and 20.

be related to diencephalic dysfunction. Moreover, variability among sibs was present in two of these families (Families DMJD-1592 and DMJD-1846), which might be due to the effect of the malformation or mere variable expressivity. We postulate that given our six familial cases of different sexes from three unrelated consanguineous families, DMJD appears to follow an autosomal recessive mode of inheritance. Genetic approaches should make it possible to identify the cause of this condition. Currently, despite exome sequencing in these affected individuals, no obvious candidate gene has emerged, but homozygosity mapping has revealed some potential chromosomal regions of interest in Family DMJD-1592 (Fig. 6). With further identification of such patients, the genetic basis and phenotypic presentation of DMJD should become clearer, and provide further insight to understanding this developmental brain disorder.

Acknowledgements

We are grateful to the patients and their families for participation.

Funding

The California Institute of Regenerative Medicine (to N.A.); the Division of Paediatric Neurology, Rady Children's Hospital, San Diego (to A.G.P.). Work in the Gleeson, Dobyns and Barkovich lab is supported by the US National Institutes of Health (R01NS048453, P01HD070494 to J.G.G.; R01NS058721 to W.B.D.; R01NS046432 to A.J.B.; RC2DA29475, R01EB00790, R01HD061414, P50NS022343, P50MH081755, R01AG031224 to A.M.D.). J.G.G. is an investigator with the Howard Hughes Medical Institutes.

References

Barkovich AJ, Millen KJ, Dobyns WB. A developmental classification of malformations of the brainstem. Ann Neurol 2007; 62: 625–39.

Barkovich AJ, Millen KJ, Dobyns WB. A developmental and genetic classification for midbrain-hindbrain malformations. Brain 2009; 132(Pt 12): 3199–230.

Barth PG, Majoie CB, Caan MW, Weterman MA, Kyllerman M, Smit LM, et al. Pontine tegmental cap dysplasia: a novel brain malformation with a defect in axonal guidance. Brain 2007; 130 (Pt 9): 2258–66.

Brain Development Cooperative Group (BDCG). Total and regional brain volumes in a population-based normative sample from 4 to 18 years: the NIH MRI study of normal brain development. Cereb Cortex 2012; 22: 1–12.

Cassandrini D, Biancheri R, Tessa A, Di Rocco M, Di Capua M, Bruno C, et al. Pontocerebellar hypoplasia: clinical, pathologic, and genetic studies. Neurology 2010; 75: 1459–64.

Cohen NR, Taylor JS, Scott LB, Guillery RW, Soriano P, Furley AJ. Errors in corticospinal axon guidance in mice lacking the neural cell adhesion molecule L1. Curr Biol 1998; 8: 26–33.

Dobson CB, Villagra F, Clowry GJ, Smith M, Kenwrick S, Donnai D, et al. Abnormal corticospinal function but normal axonal guidance in human L1CAM mutations. Brain 2001; 124 (Pt 12): 2393–406.

Engle EC. Human genetic disorders of axon guidance. Cold Spring Harb Perspect Biol 2010; 2: a001784.

Hagler DJ Jr, Ahmadi ME, Kuperman J, Holland D, McDonald CR, Halgren E, et al. Automated white-matter tractography using a probabilistic diffusion tensor atlas: application to temporal lobe epilepsy. Hum Brain Mapp 2009; 30: 1535–47.

Jovicich J, Czanner S, Greve D, Haley E, van der Kouwe A, Gollub R, et al. Reliability in multi-site structural MRI studies: effects of gradient non-linearity correction on phantom and human data. Neuroimage 2006; 30: 436–43.

Jen JC, Chan WM, Bosley TM, Wan J, Carr JR, Rub U, et al. Mutations in a human ROBO gene disrupt hindbrain axon pathway crossing and morphogenesis. Science 2004; 304: 1509–13.

Martinez S, Crossley PH, Cobos I, Rubenstein JL, Martin GR. FGF8 induces formation of an ectopic isthmic organizer and isthmocerebellar

development via a repressive effect on Otx2 expression. Development 1999; 126: 1189–200.
Martinez S, Wassef M, Alvarado-Mallart RM. Induction of a mesencephalic phenotype in the 2-day-old chick prosencephalon is preceded by the early expression of the homeobox gene en. Neuron 1991; 6: 971–81.
Mori S, van Zijl PCM, Oishi K, Faria AV. MRI atlas of human white matter. Elsevier Academic Press: London; 2011.
Nakamura H, Watanabe Y. Isthmus organizer and regionalization of the mesencephalon and metencephalon. Int J Dev Biol 2005; 49: 231–5.
Namavar Y, Barth PG, Kasher PR, van Ruissen F, Brockmann K, Bernert G, et al. Clinical, neuroradiological and genetic findings in pontocerebellar hypoplasia. Brain 2011; 134(Pt 1): 143–56.
Parisi MA. Clinical and molecular features of Joubert syndrome and related disorders. Am J Med Genet C Semin Med Genet 2009; 151C: 326–40.
Rossi A, Catala M, Biancheri R, Di Comite R, Tortori-Donati P. MR imaging of brain-stem hypoplasia in horizontal gaze palsy with progressive scoliosis. AJNR Am J Neuroradiol 2004; 25: 1046–8.
Sattar S, Gleeson JG. The ciliopathies in neuronal development: a clinical approach to investigation of Joubert syndrome and Joubert syndrome-related disorders. Dev Med Child Neurol 2011; 53: 793–8.
Scholpp S, Lohs C, Brand M. Engrailed and Fgf8 act synergistically to maintain the boundary between diencephalon and mesencephalon. Development 2003; 130: 4881–93.
Seelow D, Schuelke M, Hildebrandt F, Nurnberg P. HomozygosityMapper–an interactive approach to homozygosity mapping. Nucleic Acids Res 2009; 37 (Web Server issue): W593–9.
Yachnis AT, Rorke LB. Neuropathology of Joubert syndrome. J Child Neurol 1999; 14: 655–9; discussion 69–72.